3P5-10

Proceedings of Symposium on Ultrasonic Electronics, Vol. 35 (2014) pp. 527-528
3-5 December, 2014

Probability image of tissue characteristics based on multi-Rayleigh model for liver fibrosis by removing non-speckle signal

非スペックル信号を除去したマルチレイリーモデルによる肝組織性状確率画像

Shohei Mori[1‡], Shinnosuke Hirata[1], Tadashi Yamaguchi[2], and Hiroyuki Hachiya[1]
([1]Tokyo Tech, [2]Chiba Univ.)
森翔平[1‡]，平田慎之介[1]，山口匡[2]，蜂屋弘之[1]　([1]東工大，[2]千葉大)

1. Introduction

We have been developing a quantitative diagnostic method for liver fibrosis using ultrasound image. [1-3] In the previous study, we have proposed a multi-Rayleigh model to express a probability density function (PDF) of echo amplitude and examine a probability imaging method of tissue characteristics based on multi-Rayleigh model.[1,2] In the analysis for clinical data, we found that an approximation accuracy of multi-Rayleigh model decreases when a non-speckle signals are contained in a region of interest (ROI). The non-speckle signals also affect to the probability image of tissue characteristics based on multi-Rayleigh model. In this paper, we proposed the probability imaging of tissue characteristics based on multi-Rayleigh model using removal processing of non-speckle signals.

2. Amplitude distribution model of liver fibrosis

When scattered points are distributed closely and uniformly, such as the normal liver tissue, the PDF of echo envelope can be approximated by Rayleigh distribution. On the other hand, in inhomogeneous medium, such as the liver fibrosis, the PDF of echo envelope deviates from Rayleigh distribution. It is considered that fibrotic liver is composed of several tissues. We proposed the multi-Rayleigh model in which the distribution is modeled by combination of Rayleigh distributions with different variances, such as hypoechoic ($\sigma^2 = \sigma_L^2$), normal liver ($\sigma^2 = \sigma_M^2$), and fibrotic tissue ($\sigma^2 = \sigma_H^2$).[1] Rayleigh distribution is given by

$$p(x) = \frac{2x}{\sigma^2} \exp\left(-\frac{x^2}{\sigma^2}\right), \qquad (1)$$

where x, σ^2 is the echo amplitude and the variance of the echo amplitude, respectively.

The multi-Rayleigh model with three components is given by

$$p_{mix}(x) = \alpha_L p_L(x) + \alpha_M p_M(x) + \alpha_H p_H(x), \qquad (2)$$

where α_L, α_M, α_H are mixture rate of Rayleigh distribution with low, middle, and high variances, respectively.

E-mail address: mori@us.ctrl.titech.ac.jp

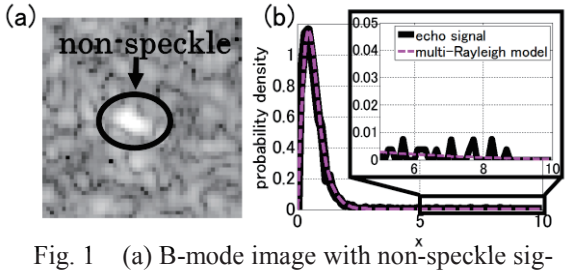

Fig. 1　(a) B-mode image with non-speckle signals. (b) Probability density function (PDF) of (a).

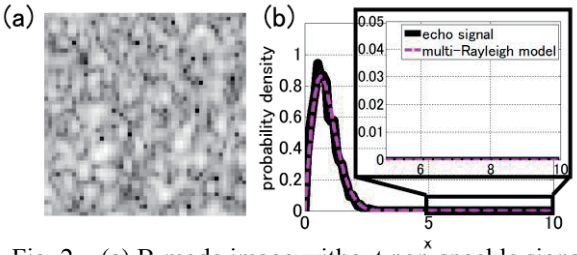

Fig. 2　(a) B-mode image without non-speckle signals. (b) PDF of (a).

3. Removal method of non-speckle signals

When the echo signals in the ROI include signals from structures which are not considered in the multi-Rayleigh model such as non-speckle structures, the PDF of the echo amplitude differs from the multi-Rayleigh model and the approximation accuracy of the multi-Rayleigh model decreases. In particular, when the non-speckle signals of high amplitude exist in the ROI (**Fig. 1(a)**), discontinuous high amplitude data appears in the PDF (**Fig. 1(b)**), and the approximation accuracy of the multi-Rayleigh model decreases. When the non-speckle signals does not exist (**Fig. 2(a)**), there does not appear the discontinuous high amplitude data in the PDF of the echo amplitude (**Fig. 2(a)**).

To extract the non-speckle signals, we focused on Kullback-Leibler (KL) divergence which was the indicator for evaluating the approximation accuracy of the model. KL divergence is given by

$$D_{KL}(P \| Q) = \sum_x P(x) \log_2 \frac{P(x)}{Q(x)}, \qquad (3)$$

where $P(x)$ is the PDF of echo amplitude, and $Q(x)$

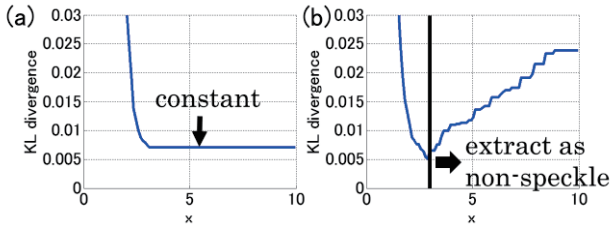

Fig. 3 KL divergence between PDF of data and multi-Rayleigh model shown in (a) Fig. 2(b) and (b) Fig. 1(b) calculated from data with amplitude less than x.

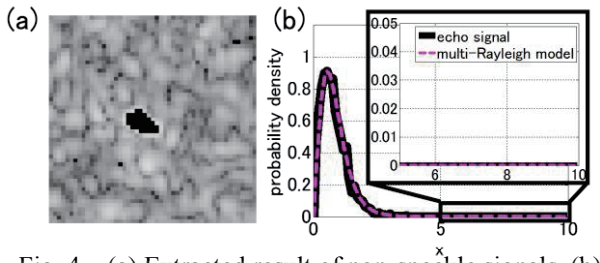

Fig. 4 (a) Extracted result of non-speckle signals. (b) PDF of (a) after removing non-speckle signals.

is the model. In this study, $Q(x)$ is the multi-Rayleigh model. When the difference between $P(x)$ and $Q(x)$ becomes small, the KL divergence also becomes small, and the KL divergence equals to 0 when $P(x)$ corresponds to $Q(x)$. **Figures 3(a)** and **3(b)** show the KL divergence of Fig. 2(b) and Fig. 1(b) calculated by removing the data of the echo amplitude which is larger than x. In Fig. 3(a), the KL divergence takes a constant value where x takes large value because the data does not include non-speckle signals. However, in Fig. 3(b), we can see that the KL divergence including high amplitude data becomes large by the effect of the non-speckle signals. Then, as the non-speckle signals, we extract the high amplitude data where the KL divergence becomes large. The extracting result for Fig. 1(a) is shown in **Fig. 4(a)** by black color. The PDF of the echo amplitude after removing non-speckle signals is shown in **Fig. 4(b)**. We can see that the discontinuous high amplitude data is removed and a shape of the PDF changes compared with the PDF of the echo amplitude before removing the non-speckle signals (Fig. 1(b)).

4. Probability image of tissue characteristics

In this section, we evaluate a probability image of tissue characteristics based on the multi-Rayleigh model by removing the non-speckle signals. In the probability image of tissue characteristics, each pixel in B-mode image has probabilities being hypoechoic and fibrotic tissues respectively.[2] We show the probability image of **Fig. 5(a)** in **Figs. 5(b)** and **5(c)**. The probability image in Fig. 5(b) is calculated before removing the non-speckle signals and the probability image in Fig. 5(c) is calculated

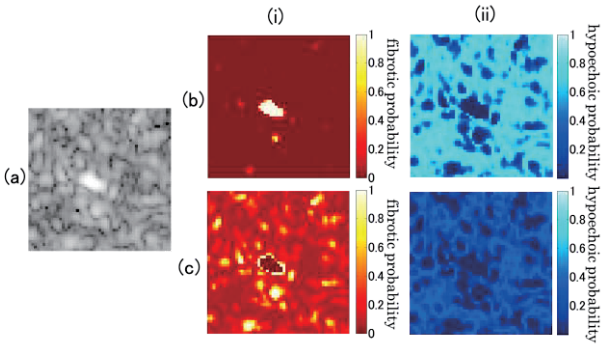

Fig. 5 (a) B-mode image. (b)(c) (i) Fibrotic and (ii) hypoechoic probability images of (a). Probability images are calculated from data (b) before removing non-speckle signals and (c) after removing.

after removing the non-speckle signals. In Figs. 5(b) and 5(c), we show the probability of fibrotic tissue in Figs. 5(b)(i) and 5(c)(i), and the probability of hypoechoic in Figs. 5(b)(ii) and 5(c)(ii) according to color bars shown in Figs. 5(b) and 5(c). From Fig. 5(b), we can see that non-speckle structures is judged as fibrotic tissue and normal liver is judged as hypoechoic by the effect of the high amplitude data of non-speckle signals. On the other hand, by removing the high amplitude data of non-speckle signals, hypoechoic probability becomes small and the pixels which are not judged as the fibrotic tissue before removing non-speckle signals are extracted as the fibrotic tissue.

5. Conclusion

In this study, we proposed the probability imaging of tissue characteristics based on multi-Rayleigh model using removal processing of non-speckle signals. The high amplitude data of non-speckle signals was judged as fibrotic tissue in the probability imaging method and the effect also appeared in the probability images of normal liver and hypoechoic tissue. Thus, we cannot obtain the probability image of tissue characteristics correctly without removal processing of non-speckle signals so that the removal of the non-speckle signals is important for quantitative evaluation of liver fibrosis.

Acknowledgement

This work was supported by KAKENHI, Grant Numbers 24103705, 25282153, and 22500433.

References

1. T. Higuchi, *et al.*: Jpn. J. Appl. Phys., **52**, No. 7, pp. 07HF19-1-6, Jul. 2013.
2. T. Higuchi, *et al.*: Jpn. J. Appl. Phys., **53**, No. 7, pp. 07KF27-1-5, Jun. 2014.
3. S. Mori, *et al.*: Jpn. J. Appl. Phys., **53**, No. 7, pp. 07KF23-1-5, Jun. 2014.